Supporting information

Cation-π interaction confined graphene oxide membrane for separation of light paraffins and olefins

Huiling Chen[a,b†], Bing Guo[c†], Dian Gong[a,b†], Jingrui Fan[a, b], Zhi Li[a], Chuhao Wang[a], Lu Wang[a,b], Chengbing Yu[d]*, Chenyu Wang [c]* and Gaofeng Zeng[a, b]*

a CAS Key Laboratory of Low-carbon Conversion Science and Engineering, Shanghai Advanced Research Institute, Chinese Academy of Sciences, Shanghai 201210, China.

b School of Chemical Engineering, University of Chinese Academy of Sciences, Beijing 100049, China

c Shanghai Ninth People's Hospital, Shanghai Jiao Tong University School of Medicine, Shanghai China

d School of Materials Science and Engineering, Shanghai University, Shanghai 200444, China.

Experiments

Membrane preparation

Asymmetric porous alumina tubes supplied by Inopor Co. (Germany) were used as support, which are 65 mm long with inner / outer diameter of 7 / 10 mm and nominal pore size of ~100 nm on the inner surface. Both ends of tube were glazed with leaving a ~30 mm middle section corresponding to 6.5 cm^2 surface area for membrane deposition.[1-3] GO powder was supplied by Xianfeng Co. (China). The precursor GO membranes were prepared by pressure filtration method. Typically, 0.2 mL GO suspension (1 mg mL^{-1}) was dispersed in 200 mL pure water by an ultrasonic disperser. Then the diluted GO suspension was driven into the lumen side of alumina tube by nitrogen in the pressure range of 2 to 10 bar.[3] The as-prepared GO membrane was dried in ambient atmosphere for 1 h.

For the ion-intercalation, the as-prepared GO membrane, which was firstly wrapped by Teflon tape on the outer surface of alumina tube, was immersed into silver tetrafluoroborate solution ($AgBF_4$, 0.5 mol L^{-1}) at room temperature for 3 h. The treated GO membrane was then rinsed with pure water before drying at 45 ^oC in vacuum for 12 h. To optimize conditions, the salt concentration (0.25-1.0 mol L^{-1}), and immersion time (0.5-3 h) were investigated. In addition, $Cu(BF_4)_2$, $NaBF_4$, and $Zn(BF_4)_2$ were employed to investigate the effects of ions on the separation performance.

Membrane separation

Gas permeation through the membranes was tested by single gas permeation method and binary isometric mixture method, respectively.[3] The membrane was fixed onto the membrane housing module with O-rings sealing on the glaze area of membrane. The gas was fed to the lumen side of the membrane. To avoid the effect of moisture on membrane, the feed gas was dehydrated by passing through a 4A molecular sieve column. The feed gas flow and pressure were controlled with a mass flow controller and a back pressure valve in the retentate line. The actual feed side pressure was measured with a pressure gauge at the retentate exit of the module. In the single gas permeation, the feed flow rate of gas was 25 mL min^{-1} and the pressure of the feed side was 0.2 bar. The permeate side was connected to the atmosphere without sweep gas. The permeate flux was measured by soap bubble flow meters with different ranges. Before flux measurement, the system was kept at the desired pressure for ca. 5 min. The permeate flux of each gas is measured at least three times.

For the binary mixture separation, two types of gas were well mixed in the gas mixer and then fed to the membrane side with a constant flow rate of 4 mL min^{-1} for each gas and the total pressure of the feed side was kept at 0.2 bar. In the permeate side, argon was introduced from one end of membrane with a constant flow rate of 25 mL min^{-1} and used as sweep gas. The permeate stream with sweep gas was analysed on-line by a gas chromatograph (Shimazu 2014C). The total flux on the permeate side was measured with a soap bubble flow meter. When the feed gas was changed, the shell side of the module was purged with the corresponding feed gas first and the flux measurements were carried out at least 10 min later.

The membrane performance was evaluated by the permeance (J, mol m^{-2} s^{-1} Pa^{-1}), ideal selectivity for single gases (IS) and separation factor (α) for gas mixtures, as expressed in equations (1)-(3):

$$J = \frac{PV}{RT} \times \frac{1}{A} \times \frac{1}{t} \times \frac{1}{\Delta P} \quad (1)$$

$$IS = \frac{J_{fast\ gas}}{J_{slow\ gas}} \quad (2)$$

$$\alpha = \frac{C_{fast\ component}}{C_{slow\ component}} \times \frac{C_{0\ slow\ component}}{C_{0\ fast\ component}} \quad (3)$$

Where P (Pa) and T (K) are the pressure and temperature on the permeate side, R is the ideal gas constant, A is the membrane area (~$6.5*10^{-4}$ m^2), t (s) is the permeation time, ΔP (Pa) is the pressure difference and C_i and C_{0i} are the component concentration on the permeate and feed side, respectively.

Characterization

The morphology and structure of membranes were characterized by scanning electron microscope (SEM, Zeiss SUPRA 55 SAPPHIRE), transmission electron microscope (TEM, JEM-2100) and X-ray diffractometer (XRD, Rigaku Ultima IV). The surface chemistry of the membranes was analysed by X-ray photoelectron spectroscopy (XPS, Thermo Fisher, K-Alpha). This included sputter depth profiling using Ar^+ ions with 30 ° beam incidence. The ion gun was operated at 3×10^{-6} Pa, 2 keV and 45 μAcm^{-2}. The elemental distribution was mapped by an energy dispersive spectrometer (EDS) attached onto SEM (Oxford Instrument). Gas sorption isotherms were measured at 298 K with a Micromeritics Instrument Corporation model 3Flex surface

characterization analyser. The carbon state was determined by Raman spectroscopy (Chameleon He-Ne laser generator with λ=531.6 nm).

Figures

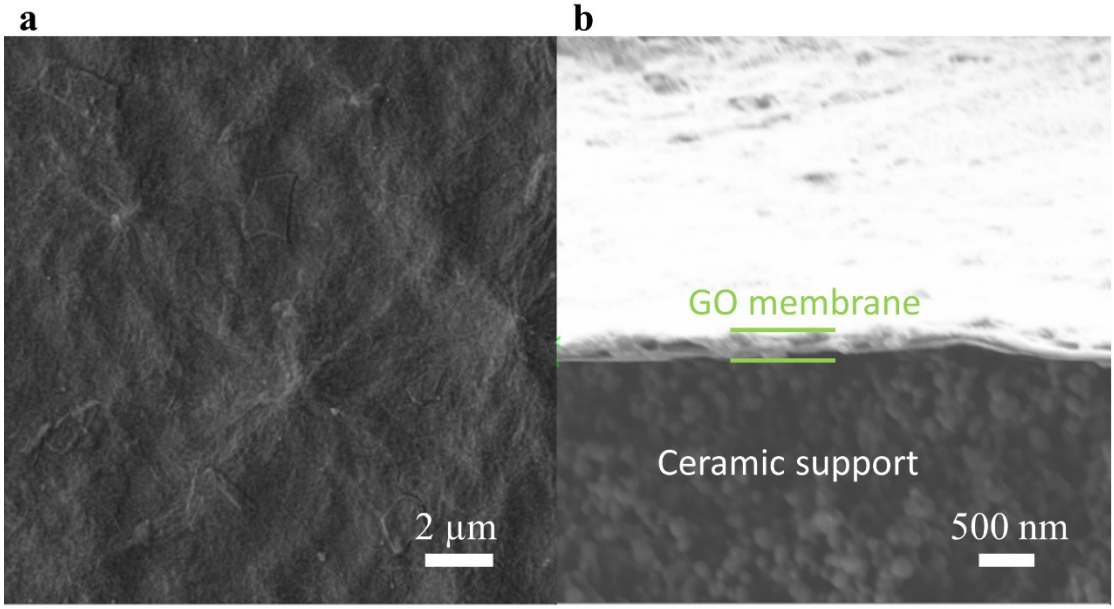

Figure S1. SEM images of (a) surface and (b) cross section of GO membrane before ions treatment.

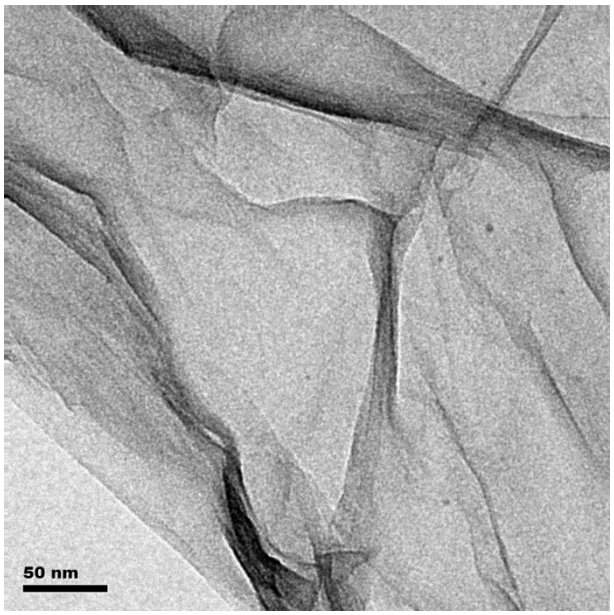

Figure S2. TEM image of the fragment of $AgBF_4$ treated GO membrane.

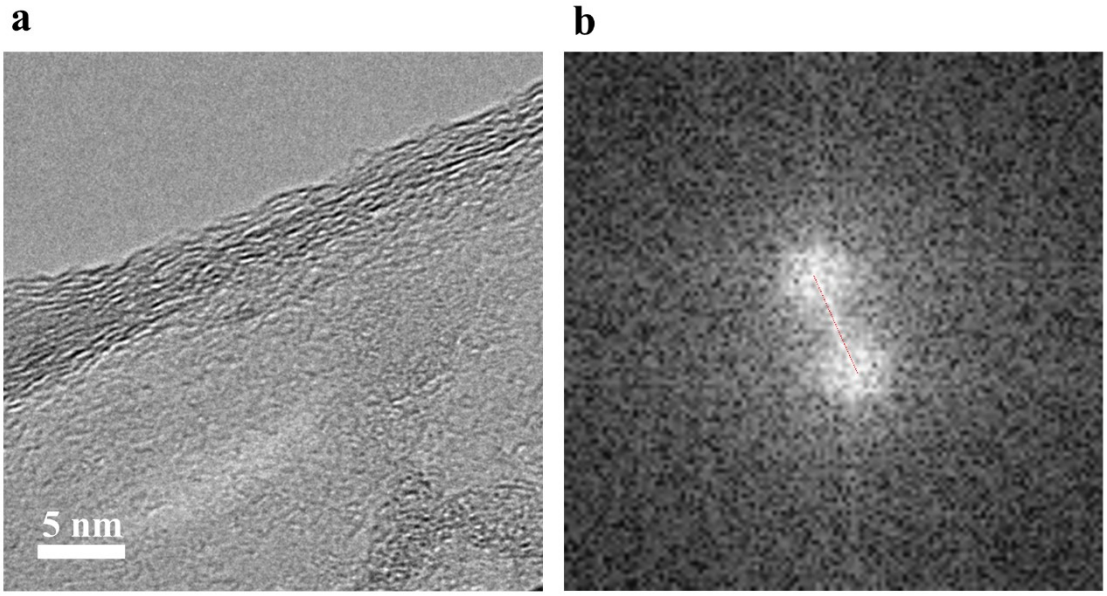

Figure S3. (a) TEM image of $Cu(BF_4)_2$ treated GO membrane fragment and (b) the Fast Fourier Transform (FFT).

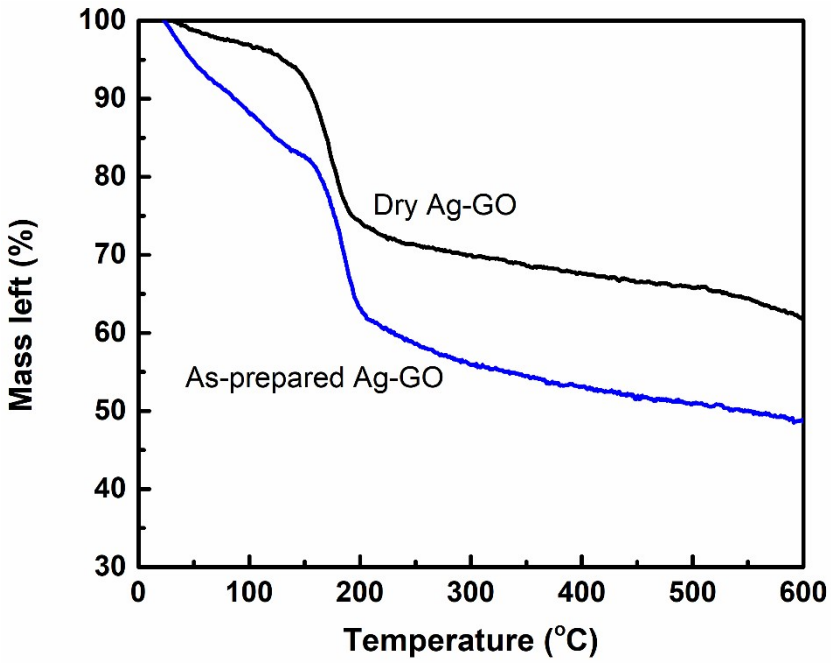

Figure S4. TGA analysis of as-prepared Ag-GO sample and the dry (45 °C in vacuum for 12 h) Ag-GO sample in Ar.

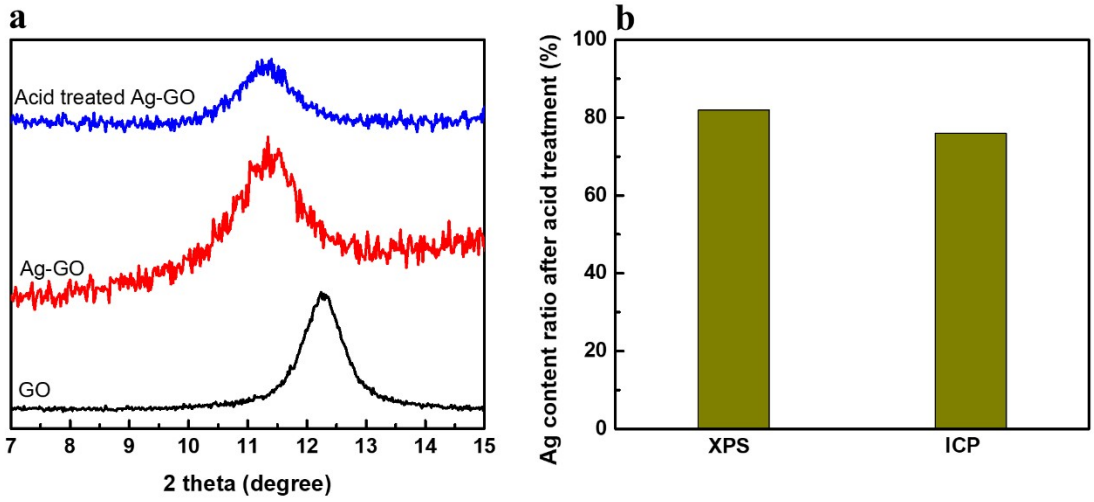

Figure S5. (a) XRD patterns of GO membrane, and Ag-GO membrane before and after acid treatment (immersion in 0.02 mol L^{-1} HNO_3 solution for 30 min), and Ag content left ratio of the acid treated Ag-GO samples with XPS and ICP measurements.

the Ag-GO membrane samples were treated in HNO_3 solution for 30 minutes. The Ag-GO samples were measured by XRD before and after the acid treatment. The peak position slightly shifted from 11.24 ° for the untreated Ag-GO to 11.46 ° for the acid treated Ag-GO sample. This reveals that most of Ag ions were remained after the acid treatment, suggesting the relatively strong interaction of cation-π effects (Figure S5a). In addition, the elemental analysis of Ag-GO samples showed that ~76-82% Ag content was kept after the acid treatment (Figure S5b), in line with the XRD results.

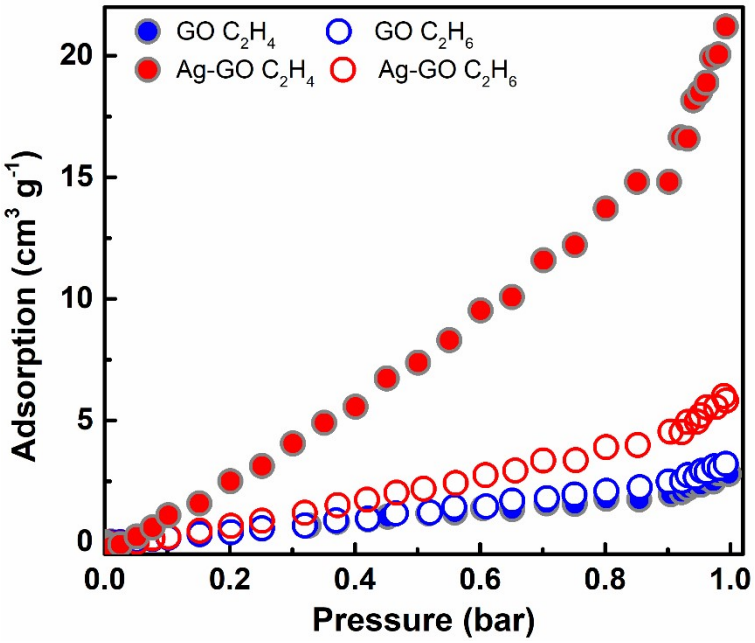

Figure S6. Adsorption isotherms of ethane and ethylene on GO membrane and Ag-GO membrane at 298 K.

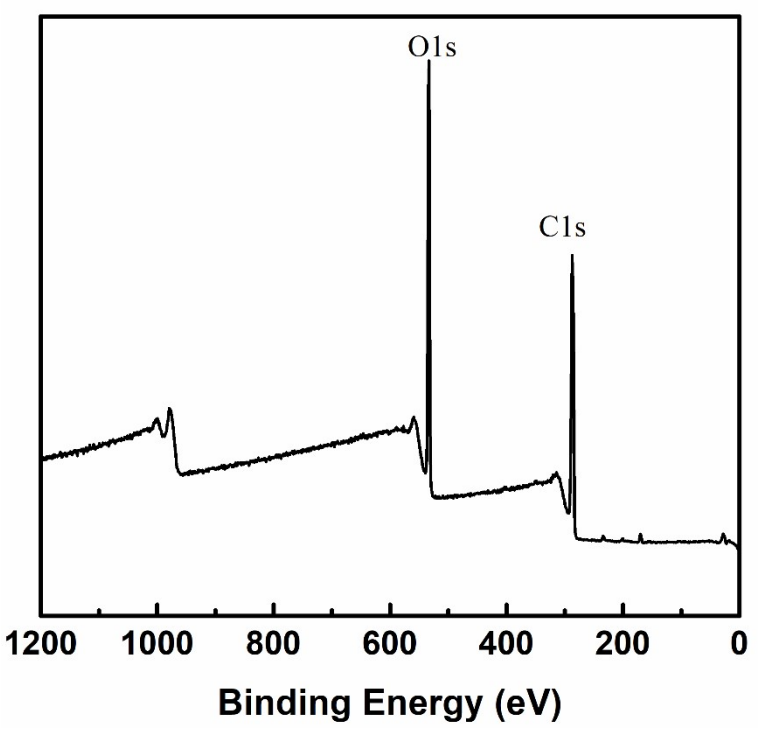

Figure S7. XPS survey spectrum of GO membrane.

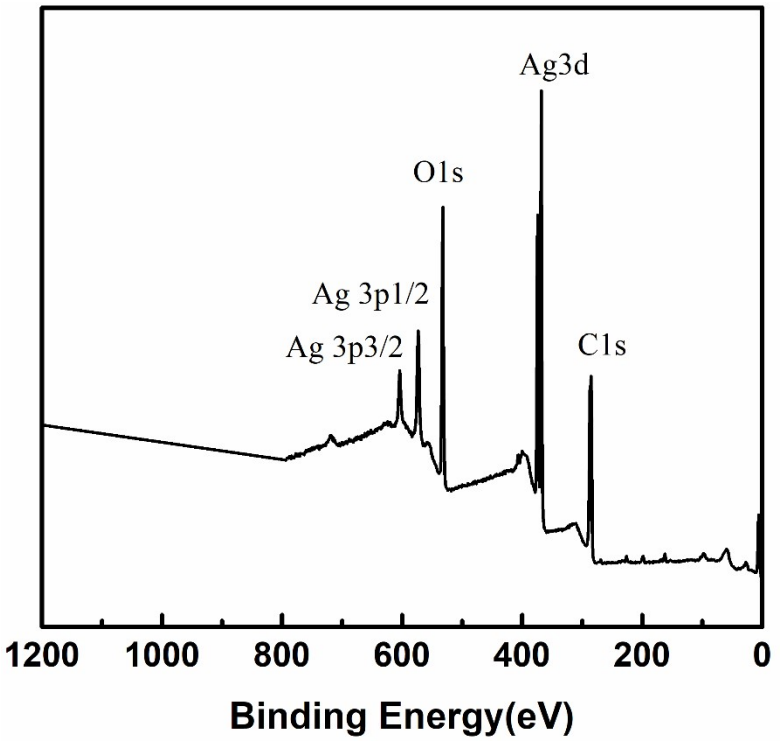

Figure S8. XPS survey spectrum of Ag-GO membrane.

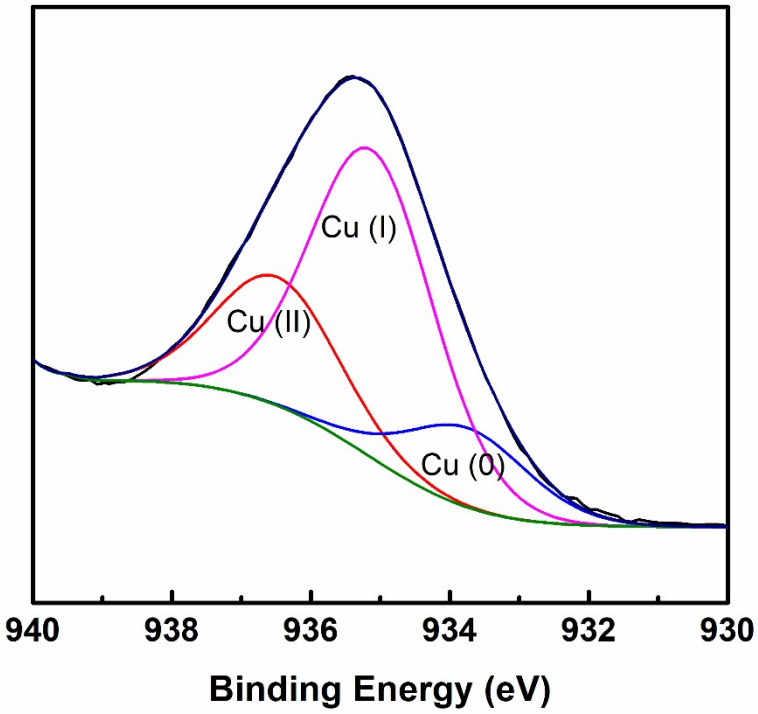

Figure S9 XPS Cu 2p spectrum of Cu-GO membrane.

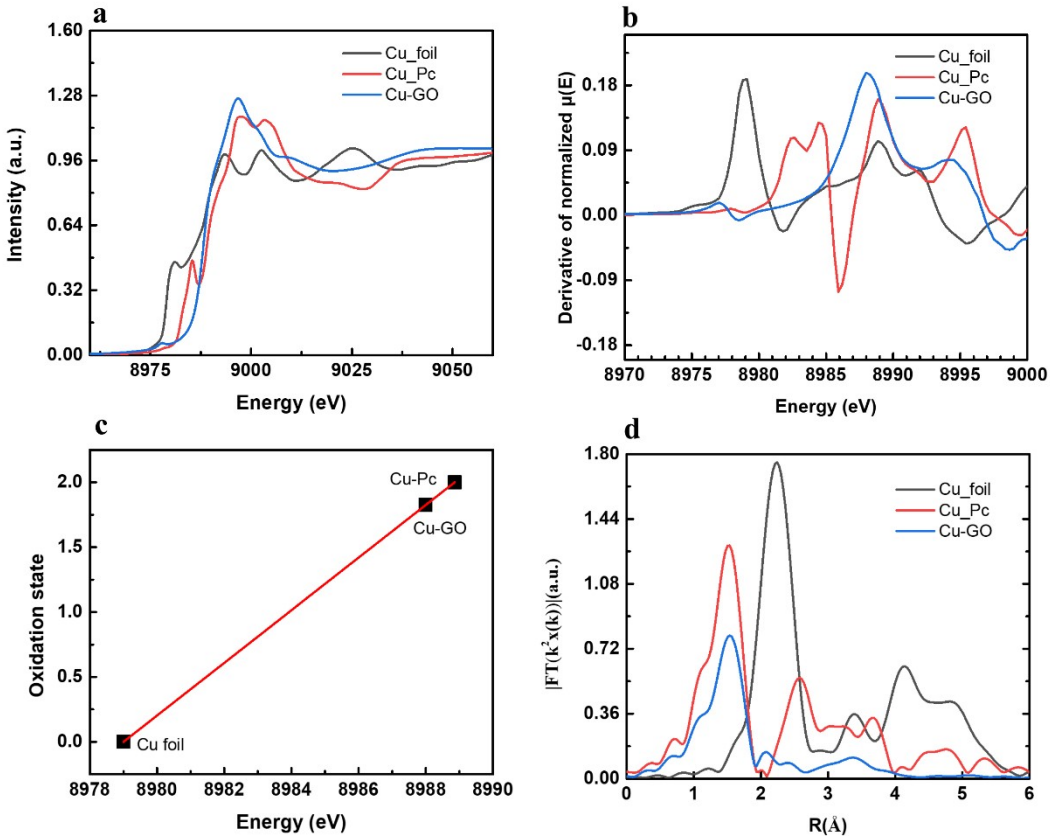

Figure S10. (a) Cu K-edge XANES, (b) First derivation of the Cu K-edge XANES, (c) Oxidation state, and (d) Fourier-transformed k3-weighted EXAFS spectra for Cu K-edge of Cu foil (Cu 0), Cu-phthalocyanine (Pc) (Cu II) and Cu-GO.

The synchrotron X-ray absorption spectroscopy (XAS) was performed for exploring the local coordination environments and evaluated the copper oxidation states. As shown in Figure S10a, the X-ray absorption near edge structure (XANES) spectra of Cu K-edge is characterized by the strong white-line peak that correspond to transition from the occupied Cu 1s to unoccupied Cu 4p. The oxidation states of the Cu atoms were further determined from the position of the rising edge of the Cu K-edge XANES, that was determined by the peak position of the first-derivative spectrum (Figure S10b). The valence states of Cu-GO sample can be estimated quantitatively as +1.83 by

plotting the standard curve that obtained from the Cu foil (0) and CuPc (+2) (Figure S10c). It is consistent with the XPS results. Moreover, the extended X-ray absorption fine structure (EXAFS) spectra was displayed as Figure S10d. The main peak of Cu-GO sample was located at 1.55 Å, which closes to that of CuPc (1.59 Å). It means the similar coordination atoms in the first shell. It was speculated to the graphene layers provided the interaction sites for Cu atoms for Cu-GO sample. It was not observed other peaks in FT-EXAFS that confirmed the atomically Cu ion was high dispersed among the graphene layers.

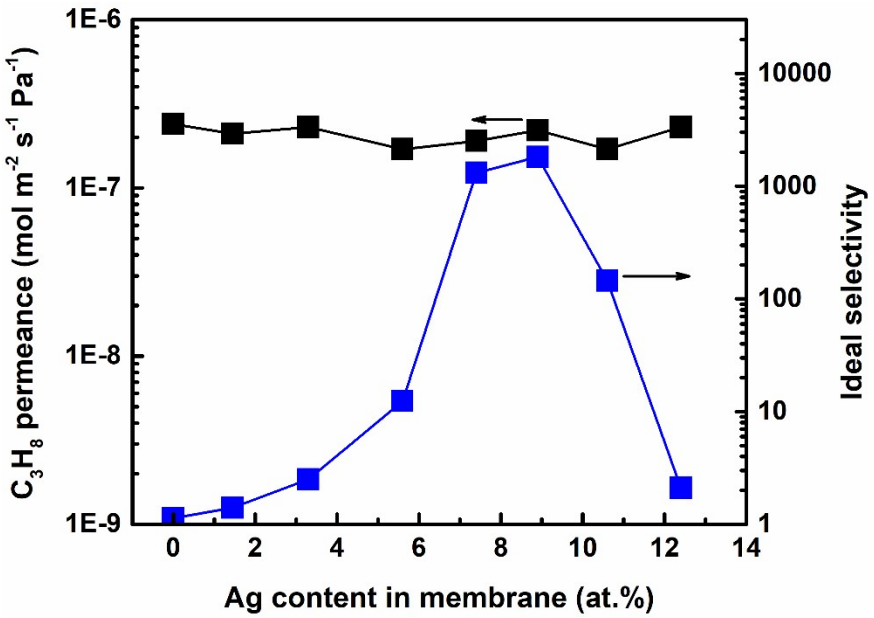

Figure S11. Effects of Ag content on the permeance and ideal selectivity.

As shown in Figure S11, the C_3H_8 fluxes are fluctuated in the range of 1.6 to 2.4 × 10^{-7} mol m^{-2} s^{-1} Pa^{-1} on the Ag-GO membranes with Ag content of 0 to 12.4 at.%. The ideal selectivity of C_3H_8/C_3H_6 is increased from 1.1 on GO membrane to 12.5 on 5.6 at.% Ag-GO membrane, then rapidly to 1310 and 1820 for 7.4 at.% and 8.9 at.% Ag-GO membranes. However, further increasing Ag content would induce the formation of salt crystals, which leads to the significantly reduce of separation performance.

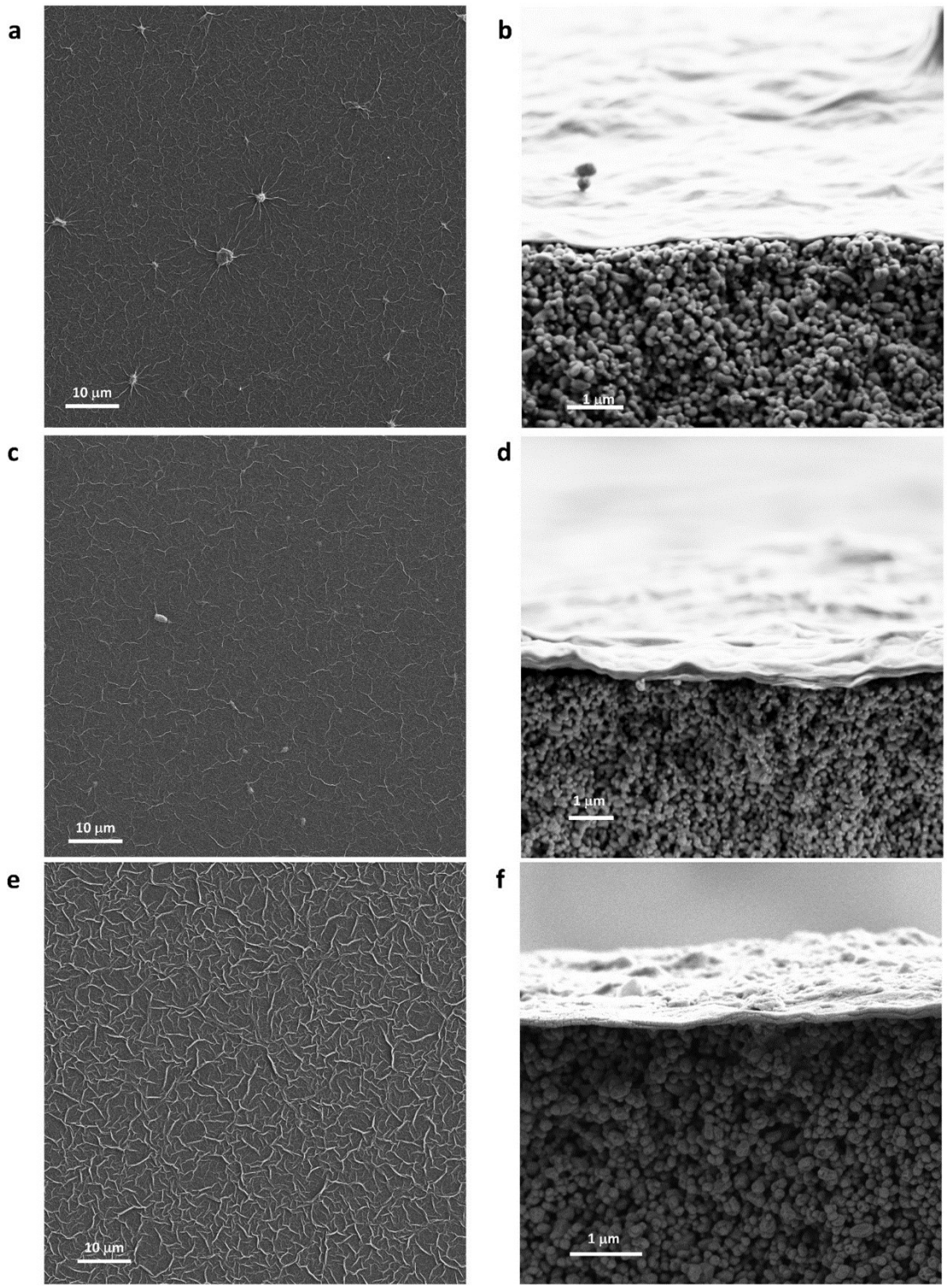

Figure S12. SEM images of surface (a, c, e) and cross-section (b, d, f) of Ag-GO membranes prepared by using (a, b) 1 µm, (c, d) 5-8 µm, and (e, f) 20 µm GO flakes.

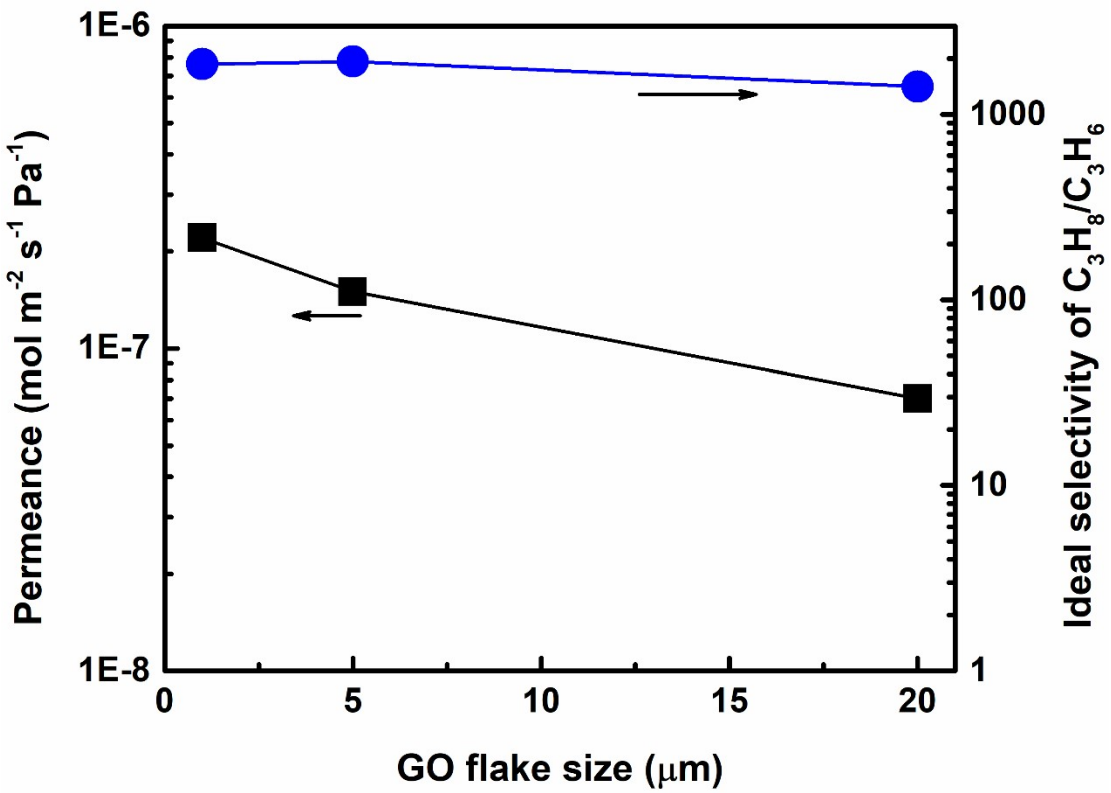

Figure S13. Effects of GO flake size on the permeation performance of C_3H_8 and C_3H_6.

Effects of GO nanosheet size on the structure and performance were investigated by using three kinds of GO powders with size of ~ 1 mm, ~ 5 mm and ~ 20 mm to prepare Ag-GO membranes.

Figure S12 show the morphology and structure of these three Ag-GO membranes. With the increase of GO size, all membrane surfaces are well covered by GO layers, but the surface wrinkles become thicker and clearer. The cross-sectional views of Ag-GO membranes display the well-packed 2D lamellar structure. Under the same preparation conditions, the thickness of Ag-GO membrane is well controlled in the range of ~150 - 250 nm.

These Ag-GO membranes containing various GO flakes were tested by using single gas

method (Figure S13). With the increase of GO flake, C_3H_8 permeance decreased from 2.2×10^{-7} mol m^{-2} s^{-1} Pa^{-1} of 1 μm flakes to 7.1×10^{-8} mol m^{-2} s^{-1} Pa^{-1} of 20 μm flakes. This may contribute to that the smaller flakes can provide more entrances, which is consistent with the reported results.[4] On the other hand, the ideal selectivities over these membranes are all higher than 1200, indicating that the Ag intercalation structure is well established in these membranes.

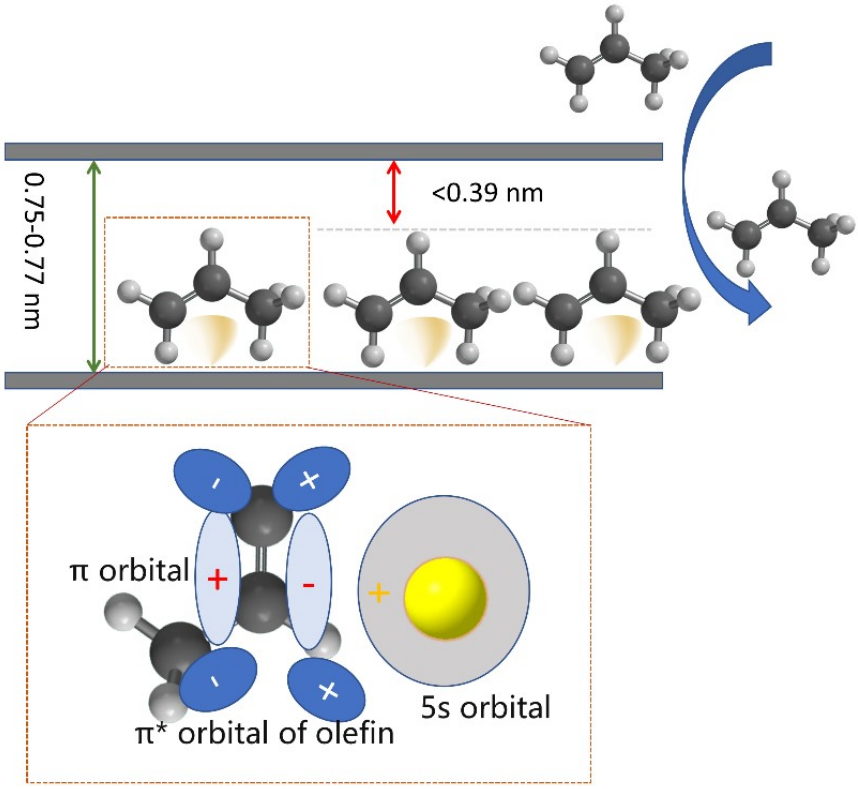

Figure S14. Schematic of the exclusion mechanism of propene on the 2D channel of Ag-GO membrane.

The XRD results reveal that the 2D channel size of cation-GO membranes is 0.75-0.77 nm. The kinetic diameter of C_2H_4/C_2H_6 and C_3H_6/C_3H_8 are 0.39 nm and 0.43 nm, respectively. Therefore, the molecule layer number in the membrane are less than 2 for all these gases. When the fixed cations have the capacity of selective adsorption, the adsorbed C_2H_4 or C_3H_6 occupied 1 molecule layer spacing, leaving the unoccupied spacing that smaller than the size of C_2H_4 and C_3H_6 (Figure S14). Therefore, the permeance of C_2H_4 and C_3H_6 is small. As the weak interactions between metal ions and paraffins, at least 1 molecule layer of C_2H_6 or C_3H_8 can pass through the membrane smoothly, leading to high permeance of paraffins. Therefore, the fast permeance of paraffin and the slow permeance of olefins result in high ideal selectivity. In the case

of binary mixture, both paraffin and olefin molecules can pass through the membrane. The co-existed paraffin impacts the adsorption effects of olefin and the diffusion of paraffin further suppress the adsorption amount of olefin molecules. Therefore, the separation factor on binary mixture is significantly declined.

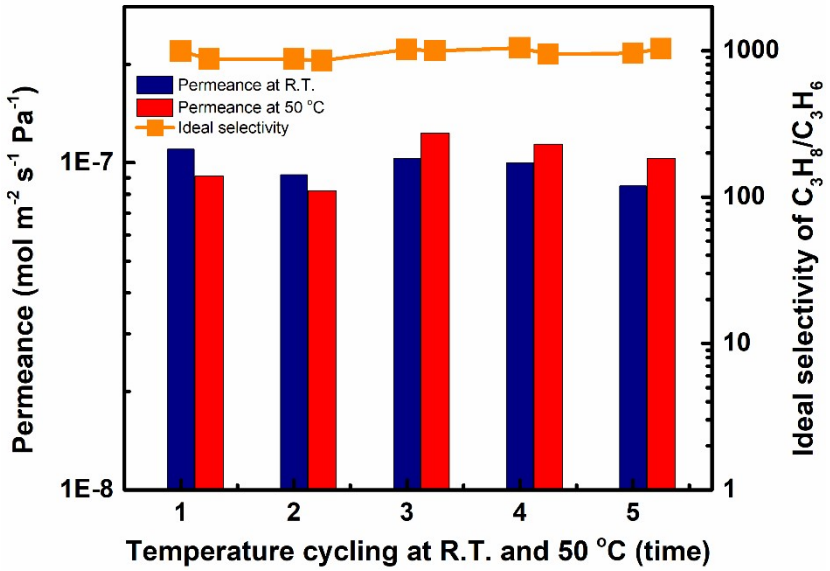

Figure S15. Permeance performance of Ag-GO membrane in the temperature cycling between room temperature and 50 °C.

The thermal stability of Ag-GO membrane was investigated by testing the permeance performance at the cycling temperature between room temperature and 50 °C for 5 times. During each temperature cycling, the Ag-GO membrane delivered similar C_3H_8 fluxes (~1.0 × 10^{-7} mol m^{-2} s^{-1} Pa^{-1}) and ideal selectivity (~960) with reasonable fluctuations at room temperature and 50 °C (Figure S15).

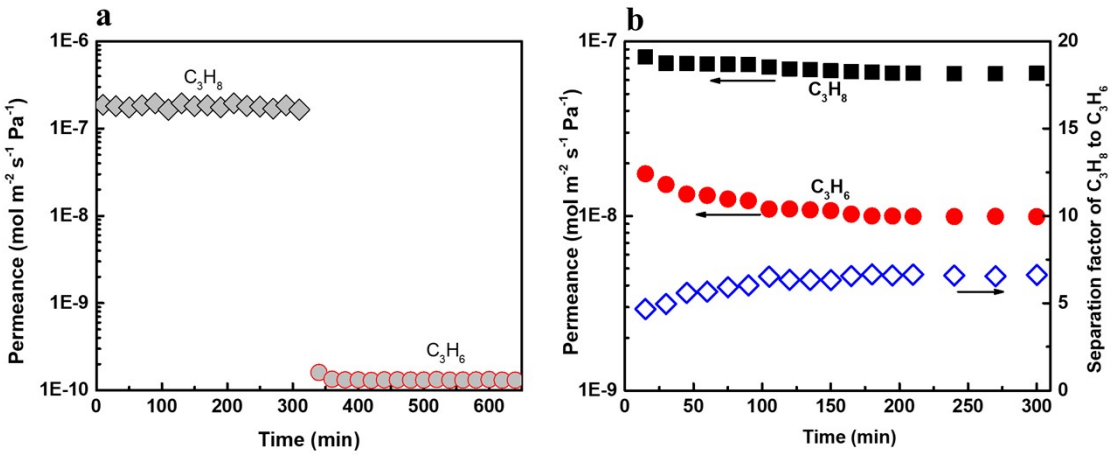

Figure S16. Stability tests of (a) single gas method and (b) 1:1 mixture method.

As shown in Figure S16, the Ag-GO membrane exhibits stable C_3H_8 permeance of 1.8×10^{-7} mol m^{-2} s^{-1} Pa^{-1} with slight fluctuations in 300 min by using the single gas feeding method. In addition, the C_3H_6 permeance was declined from 1.6×10^{-10} mol m^{-2} s^{-1} Pa^{-1} to 1.3×10^{-10} mol m^{-2} s^{-1} Pa^{-1} in the first 20 min and then kept around 1.3×10^{-10} mol m^{-2} s^{-1} Pa^{-1} in the following 300 min, reflecting the ideal selectivity of C_3H_8/ C_3H_6 always > 1100. For the stability test with 1:1 binary mixture, C_3H_8 permeance of Ag-GO membrane is stable around 7×10^{-8} mol m^{-2} s^{-1} Pa^{-1} and C_3H_6 permeance is firstly decreased from 1.7×10^{-8} mol m^{-2} s^{-1} Pa^{-1} to 1.3×10^{-8} mol m^{-2} s^{-1} Pa^{-1} and then kept stable around 1.1×10^{-8} mol m^{-2} s^{-1} Pa^{-1} in a 300 min test, which delivers the separation factors of C_3H_8/C_3H_6 in a narrow range of 4.7 to 6.6.

Reference

1. D. Gong, Y. Yin, H. Chen, B. Guo, P. Wu, Y. Wang, Y. Yang, Z. Li, Y. He and G. Zeng, *ACS Nano*, 2021, **15**, 9871-9881.
2. G. Zeng, Y. Wang, D. Gong, Y. Zhang, P. Wu and Y. Sun, *ACS Cent Sci*, 2019, **5**, 1834-1843.
3. J. Yang, D. Gong, G. Li, G. Zeng, Q. Wang, Y. Zhang, G. Liu, P. Wu, E. Vovk, Z. Peng, X. Zhou, Y. Yang, Z. Liu and Y. Sun, *Adv Mater*, 2018, **30**, e1705775.
4. H. W. Kim, H. W. Yoon, S. M. Yoon, B. M. Yoo, B. K. Ahn, Y. H. Cho, H. J. Shin, H. Yang, U. Paik, S. Kwon, J. Y. Choi and H. B. Park, *Science*, 2013, **342**, 91-95.